Applied Biochemistry and Biotechnology (2024) 196:701–716
https://doi.org/10.1007/s12010-023-04492-z

ORIGINAL ARTICLE

Chitosan-Albumin Nanocomposite as a Promising Nanocarrier for Efficient Delivery of Fluconazole Against Vaginal Candidiasis

Morvarid Hatamiazar[1] · Javad Mohammadnejad[2] · Sepideh Khaleghi[1]

Accepted: 11 April 2023 / Published online: 13 May 2023

Abstract

Currently, the high incidence of fungal infections among females has resulted in outstanding problems. Candida species is related with multidrug resistance and destitute clinical consequences. Chitosan-albumin derivatives with more stability exhibit innate antifungal and antibacterial effects that boost the activity of the drug without inflammatory impact. The stability and sustained release of Fluconazole in mucosal tissues can be ensured by encapsulating in protein/polysaccharide nanocomposites. Thus, we developed chitosan-albumin nanocomposite (CS-A) loaded with Fluconazole (Flu) antifungals against vaginal candidiasis. Various ratios of CS/Flu (1:1, 1:2, 2:1) were prepared. Thereafter, the CS-A-Flu nanocomposites were qualified and quantified using FT-IR, DLS, TEM, and SEM analytical devices, and the size range from 60 to 100 nm in diameter was attained for the synthesized nanocarriers. Afterward, the antifungal activity, biofilm reduction potency, and cell viability assay were performed for biomedical evaluation of formulations. The minimum inhibitory concentration) and minimum fungicidal concentration on *Candida albicans* were attained at 125 ng/μL and 150 ng/μL after treatment with a 1:2 (CS/Flu) ratio of CS-A-Flu. The biofilm reduction assay indicated that biofilm formation was between 0.05 and 0.1% for CS-A-Flu at all ratios. The MTT assay also exhibited excellent biocompatibility for samples, about 7 to 14% toxicity on human HGF normal cells. These data have indicated that CS-A-Flu would be a promising candidate against *Candida albicans*.

Keywords Chitosan-albumin nanocomposite · Fluconazole · Vaginal candidiasis · Antifungal activity · Biofilm reduction · Biocompatibility

✉ Sepideh Khaleghi
s.khaleghi@iautmu.ac.ir

[1] Department of Biotechnology, Faculty of Advanced Science and Technology, Tehran Medical Sciences, Islamic Azad University, Tehran 1916893813, Iran

[2] Department of Life Science Engineering, Faculty of New Sciences and Technologies, University of Tehran, Tehran, Iran

Introduction

The ever-increasing prevalence of fungal infections among people has received more attention throughout the world. It has been reported that relatively 1.2 billion people per year have been infected with fungal diseases during the last decades which is significantly a considerable amount [1, 2]. The overuse of the most potential antifungals such as azole antifungals groups (fluconazole (Flu), ketoconazole, miconazole, tioconazole, itraconazole, etc.) has been resulted in causing drug resistance among *Candida* species and made further hurdles in treatment and suppression of candida vaginitis [3]. As a result, novel types of antifungals are needed to avoid the disadvantage of the conventional treatment approaches and therapeutics.

An efficient procedure for the treatment of fungal infections is developing drug delivery systems (DDSs) based on nano-sized materials that could significantly improve the antifungal performance of therapeutics [4, 5]. Among different fabricated nanomaterials, polymeric nanoparticles are contemplated as a practical candidate for increasing the antifungals' half-life through various routes [6]. Chitosan nanoparticles, made of poly [β-(1-4)-linked-2-amino-2-deoxy-D-glucose] units, are one of the excellent platforms for the delivery of drugs against vaginal candidiasis [7]. These polymeric nanoparticles have several merits, including having enough core cavity for encapsulating a high amount of antifungals, sustained drug release, ease of synthesis, biocompatibility, protecting drugs from enzymatic degradation, having a tunable size, enhancement of water solubility of antifungals, boosting the stability of therapeutics, and so on [8, 9]. Moreover, possession of the accessible functional groups on the surface of CS is provided a great opportunity for surface modification goals which could play a crucial role in raising the positive properties of CS nanoparticles in DDSs [10]. The positive surface charge of CS (owing to amine groups) can also react with the negative charge of the surface of fungi and lead to suppression of their growth [11]. Albumin is one of the elements which can be conjugated with CS nanoparticles in the form of nanocomposite. Albumin is a negatively charged protein that boosts the stability of nanoparticles and limits immunological identification of nanocarriers by absorbing water and establishing a space repulsion. [12, 13]. Albumin can also serve as an anti-inflammatory and antioxidant element in the human body [14]. Great biocompatibility, biodegradability, stability, solubility, etc. are considered other aspects of this protein that made it a potential candidate for DDS. Albumin contain many different types of functional groups and hence have the capacity to bind and transport large amounts of medication via various processes such as electrostatic contacts, hydrophobic interactions, and covalent connections [15]. Albumin, an acidic protein, is very soluble and stable in a wide range of pH and for a long time at high temperatures and also in organic solvents which is a suitable subunit for making nanocarriers in drug delivery [13]. Some other unique property is its enhanced uptake by inflamed tissues, which is favorable for application as a therapeutic carrier [15]. However, the main drawback regarding this protein in the delivery of therapeutics is related to its poor bioavailability after oral administration [16]. Thus, in order to overcome this deficiency, this protein can be used in combination with other nanoparticles such as CS to further exhibit the antioxidant, immunomodulation, and drug carrier ability against various diseases like vaginal candidiasis [17].

On the other hand, Flu which is the first-generation triazole antifungal, can be used as potential therapeutics against vaginal candidiasis. This drug can be led to interference in the transformation of lanosterol to ergosterol by blocking cytochrome P450 which, in turn, results in an interruption in the formation of the cell membrane in pathogenic fungi [18,

19]. Although local use of Flu is a suggested way for the treatment of candidiasis with low side effects, the oral use of Flu can prescribe in some adverse stages of the disease which is along with remarkable side effects including stomach upset, rash, diarrhea, and hepatotoxicity [20, 21]. Moreover, in some cases, local treatment is not suggested to prevent the systemic spreading of fungal infections. As a result, applying nanoparticles-based DDSs can be a promising approach to solving the side effects and problems of using pure Flu.

In this study, in order to improve CS physicochemical properties and stability and further extend its applications, CS/albumin derivative was investigated, obtained by both chemical modifications and polyelectrolyte complex formation. So, the aim of the current examination was to develop covalently and non-covalently bonded CS-albumin (A) nanocomposite loaded with Flu antifungals against vaginal candidiasis. Therefore, after the preparation of the CS-A-Flu nanocomposite and its derivatives, they were characterized with FT-IR, DLS, TEM, and SEM analytical devices to qualify and quantify the syntheses. Then the antifungal activity, biofilm reduction potency, and cell viability assay were conducted on the human normal cell to evaluate treatment efficiency and biocompatibility of the synthesized nanocomposite.

Materials and Methods

Materials and Apparatus

Bovine serum albumin (A), low molecular weight CS (50,000 to 190,000 Da; Viscosity: 20–300 cp), Flu, sodium tripolyphosphate (TPP), citric acid, and acetic acid were purchased from Sigma-Aldrich (St. Louis, MO). Also, N-hydroxysuccinimide ester (NHS) and 1-(3-dimethylaminoproply)-3-ethylcarbodiimide hydrochloride (EDC) were bought from Sigma-Aldrich. All solutions were prepared in deionized water. On the other hand, *C. albicans* ATCC 17110 and human HGF normal cells were purchased from Pasteur Institute, Tehran, Iran.

Analytical evaluation of synthesized samples was conducted via a NanoDrop 2000c UV–Vis spectrophotometer (Thermo scientific), Fourier transform infrared (FT-IR) spectrometer (Perkin-Elmer 843), dynamic light scattering (DLS) (NanoBrook 90 Plus), scanning electron microscopy (SEM) (Zeiss Evo), and transmission electron microscopy (TEM) (Philips EM 208S).

Synthesis of CS-A

The CS and A were covalently (CS-A (C)) and non-covalently (CS-A (NC)) conjugated with each other as the following procedure. The esterification reaction was used for covalent interaction between CS and A; 1.5 g of A was dissolved in 50 mL DI water and stirred for about 30 min under 50 rpm at room temperature. Then the mixture of EDC (150 mg) and NHS (250 mg) was made by solubilizing in DI water. Next, the prepared solutions were combined for the activation of A. This process was carried out under a nitrogen atmosphere and dark conditions and stirred at 50 rpm for 4 h. Afterward, the activated A was drop by drop added to the prepared CS solution containing 50 mg of CS powder suspended in 5 mL of 1% acetic acid. The reaction was implemented under stirring at 60 rpm for 7 h which continued by adding 6 mL NaOH (1 M) under stirring at room temperature. The resultant nanocomposite was centrifuged at 4000 rpm for 20 min to separate the CS-A

(C) from solvents. This nanocomposite was rinsed and centrifuged three times using DI water, and precipitation was saved at 4 °C.

On the other hand, for preparing CS-A (NC) nanocomposite, briefly, 50 mg of CS powder solubilized in 5 mL of 1% acetic acid followed by adding to the prepared A solution containing 1.5 g of A in 50 mL DI water. Thereafter, the mixture was stirred at 60 rpm and room temperature for 2 h and 6 mL NaOH (1 M) added to the mixture to completely separate reactants from the rest of the solution. Next, the mixture was centrifuged at 4000 rpm for 20 min, and the washing process was repeated for the purification of CS-A (NC) nanocomposite as same as the purification process of the CS-A (C) sample. The precipitation of CS-A (NC) and CS-A (C) samples were dissolved in 5 mL of 1% acetic acid (v/v) under vigorous stirring to obtain a homogenous solution and then slowly treated with 4 mL of 0.5% TPP solution, as a cross-linking agent, under ultrasonication conditions for 15 min for providing the spherical nanocarrier. Then, the prepared nanocomposites were collected through centrifugation at 8000 rpm for 30 min and washed with 15 mL of distilled water for three times.

Synthesis of CS-A-Flu

For the entrapment of Flu in CS-A (C) and CS-A (NC) nanocomposites, various concentrations of Flu were provided to prepare the different ratios (W/W) of CS to Flu as the following: 1:1, 1:2, and 2:1 CS/Flu. Briefly, 20 mg, 20 mg, and 40 mg of Flu were separately dissolved in 5 mL DMSO in three backers by stirring at 60 rpm for 30 min. Then, 20 mg CS-A (C), 40 mg CS-A (C), and 20 mg CS-A (C) were separately solubilized in 5 mL of 1% acetic acid which continued by mixing the prepared Flu solutions and prepared CS-A (C) solutions at the ratio of 1:1, 1:2, and 2:1. In what follows, the mixtures were separately stirred at 60 rpm and room temperature for 2 h and saved at 4 °C for 3 days. Afterward, 4 mL TPP (0.5%) solution was separately added to the prepared mixtures under ultrasonication circumstances for 15 min to attain the globular CS-A-Flu (C) nanocomposites. Subsequently, the mixture was centrifuged at 10,000 rpm for 15 min to separate unloaded Flu and free reagents in the prepared mixture. The same scenario was done for CS-A (NC) sample for preparing CS-A-Flu (NC) as well.

Characterization of Nanocomposites

Various analytical tools, including FT-IR (Fourier transform infrared spectroscopy), DLS (dynamic light scattering), SEM (scanning electron microscopy), and TEM (transmission electron microscopy) were used for qualification and quantification of the nanocomposites. FT-IR device was employed for qualification of the synthesis, drug loading, surface engineering, and deformation and formation of bonds. The wavelength ranges between 400 and 4000 cm^{-1} were applied for implementing this analysis based on the KBr pellet procedure. The second analysis was the DLS approach which was used for ascertaining the average hydrodynamic diameter of the synthesized nanocomposites. For this test, the freshly prepared suspensions of specimens were used after strong sonication via ultrasonication device at 37 °C for 15 min, and the measurement was done at 37 °C using a quartz cuvette at nM concentrations of specimens. Thirdly, the nanoparticles' size, shape, dispersity, and morphology were scrutinized using the SEM and TEM devices. The surface morphology, shape, and distribution of synthesized nanocomposites were studied via SEM after fixing specimens on the stub against carbon

adhesive tape. Then samples were sputter-coated with gold and subjected to SEM at 25 kV for assessment [22]. Regarding the TEM technique, the freshly prepared synthesized nanocomposites were exposed to strong sonication and dispersed onto a copper grid and dried at 25 °C. Afterward, after absorbing excess liquid using filter paper, the photographs of samples were taken at an accelerating voltage of 120 kV.

Antifungal Assay

The antifungal activity of the synthesized nanocomposites, including CS-A-Flu (NC), CS-A-Flu (C), and Flu were studied on *C. albicans* ATCC 17110 using the MIC (minimum inhibitory concentration) and MFC (minimum fungicidal concentration) assay. Briefly *C. albicans* ATCC 17110 was grown up on agar cup diffusion, and then various ratios (1:1, 1:2, and 2:1) of the prepared Flu/CS-A samples with different concentrations of CS-A (C1=25, C2=50, C3=75, C4=100, C5=125 and C6=150 µg CS-B/mL), and free Flu (C1=25, C2=50, C3=75, C4=100, C5=125 and C6=150 µg Flu/mL) were applied in this antifungal test. The antifungal ability of provided samples was scrutinized using a 96-well plate lysis assay as the following procedure; 0.5 McFarland concentration of *C. albicans* ATCC 17110 was prepared, seeded into 96-well plates, and incubated for 24 h at 37 °C for the attachment of cells. After growing up of the *C. albicans* ATCC 17110, the PBS was used for washing 96-well plates which continued by treating the fungal cells with the prepared nanocomposites at different ratios. Then the MIC and MFC tests were conducted at 24 h and 48 h of post-treatment times by culturing the treated samples on drug-free agar to look for survivors when the drug is diluted out [23].

Biofilm Reduction Assay

The biofilm reduction assay was implemented to investigate the ability of synthesized nanocomposites (CS-A-Flu (NC), CS-A-Flu (C), and Flu) in inhibiting *C. albicans* ATCC 17110. To achieve this, *C. albicans* ATCC 17110 strain was grown up on agar cup diffusion which followed by treatment with different concentrations of CS-A (C1=25, C2=50, C3=75, C4=100, C5=125 and C6=150 µg CS-B/mL), and free Flu (C1=25, C2=50, C3=75, C4=100, C5=125 and C6=150 µg Flu/mL) for evaluating samples' antifungal performance. Thereafter, *C. albicans* ATCC 17110 cells were washed with PBS and transferred into a 96-well microplate. The plate was incubated for 24 h at 37 °C which continued by rinsing the biofilm with PBS and treatment with the prepared nanocomposites in the well of the microplates. Next, microplates were incubated at 37 °C for 24 h, wells washed with PBS, and cells fixed by applying methanol. Biofilms were thoroughly air-dried and stained with 150 µL of 0.2% crystal violet (w/v) (Sigma-Aldrich, USA) dissolved in distilled water supplemented with 1.9% ethanol (v/v) for 10 min (RT, static). Then excess crystal violet was removed, and biofilms gently washed twice with 200 µL of PBS. Crystal violet stain that had incorporated into the biofilm was re-solubilized upon the addition of 150 µL of 1% sodium dodecyl sulphate (SDS) (w/v) (Sigma-Aldrich, USA). Plate was incubated for 10 min (RT, static). Biofilm biomass was quantified by spectrophotometrically measuring the re-solubilized crystal violet stain that had once incorporated into the sample at OD540nm (SpectraMax Plus 384 microplate reader).

Cell Culture

Human HGF normal cell line was prepared from the Pasture Institute of Iran. This cell line was cultured in the DMEM medium (Gibco, UK) supplemented with 10% FBS, 2 mM glutamine, 100 μgmL^{-1} streptomycin, and 100 IU mL^{-1} penicillin for cellular analysis.

MTT Assay

The biocompatibility effects of CS-A-Flu (NC), CS-A-Flu (C), and pure Flu were surveyed on HGF normal cells applying the MTT assay at 24 h and 48 h [24]. As same as the antifungal tests, the prepared ratios (1:1, 1:2, and 2:1) of the prepared Flu/CS-A samples with different concentrations of CS-A (C1=25, C2=50, C3=75, C4=100, C5=125 and C6=150 μg CS-B/mL), and free Flu (C1=25, C2=50, C3=75, C4=100, C5=125 and C6=150 μg Flu/mL) were used in this test as the following procedure. The synthesized nanocomposites were practically prepared in a serum-supplemented tissue culture medium, sterilized through 0.2-mm filtration at pH 7.4, 7500 cells/100 μL of HGF cells seeded in each well of 96-well microtiter plates, and microplates incubated in an incubator overnight for cell attachment. The cell culture medium of the microplates was then replaced with 100 μL of various prepared samples, and the HGF cells were incubated for another 24 h. In what follows, the medium of sample-treated wells was substituted with 200 μL DMEM without serum. Next, 20 μL of sterile-filtered MTT (3-[4,5-dimethylthiazol-2-yl]-2,5-diphenyl tetrazolium bromide) salt was solubilized in PBS at pH 7.4 (5 mg/mL) and added to each well at the concentration of 0.5 mg MTT/mL. After incubating for 4 h, the suspension liquid was collected, the HGF cells were re-suspended in DMSO, and optical density (OD) was read at 450 nm using SpectraMax Plus 384 microplate reader ($n = 3$). Eventually, the difference in OD values between the treated and non-treated cells was presented as cell viability values.

Statistical Analyses

The outputs were presented as the mean ± SD of three determinations ($n = 3$), and the analysis of variance (one-way ANOVA) was done for ascertaining the statistical significance at the 0.05 significance level.

Results and Discussion

Characterization of Nanocomposites

FT-IR Analysis

FT-IR spectroscopy technique was carried out for qualification of synthesized nanocomposites, including pure CS, CS-A (NC), CS-A (C), CS-A-Flu (NC), and CS-A-Flu (C). Figure 1 demonstrates the outputs of this analytical test. According to the results, the absorption peaks attained at around 3443 cm^{-1}, 3250 to 3340 cm^{-1}, 1164 cm^{-1}, and 1065 cm^{-1} are assigned to –NH_2 and –OH groups stretching vibration, O−H and N−H stretching

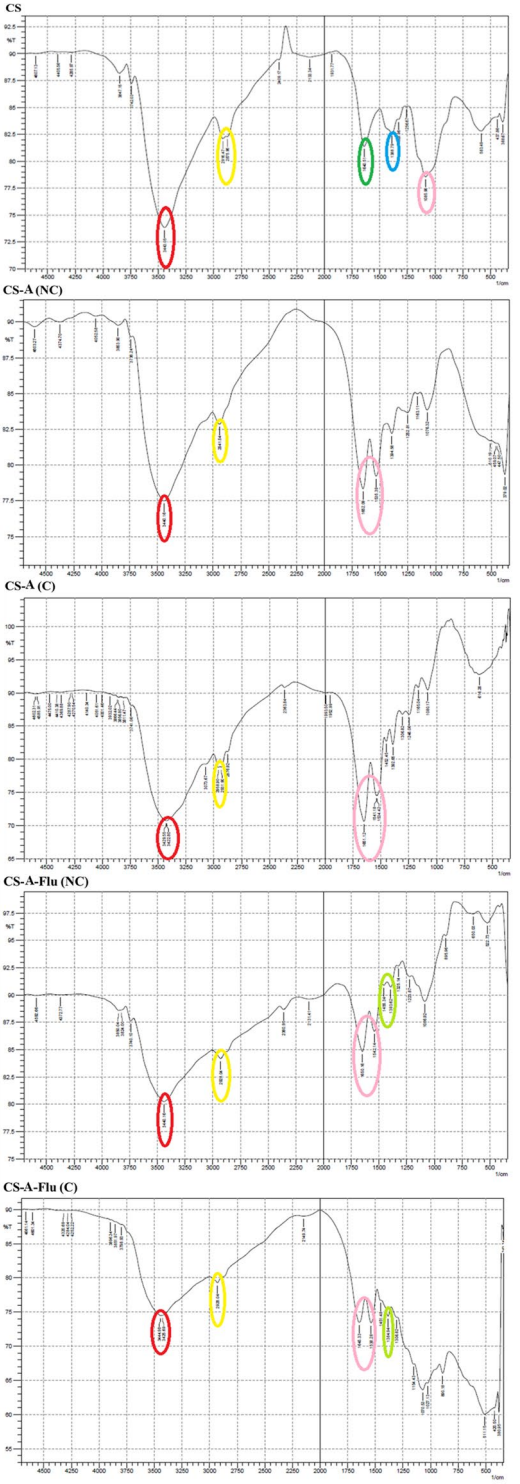

Fig. 1 The FT-IR spectra of CS, CS-A (NC), CS-A (C), CS-A-Flu (NC), and CS-A-Flu (C). As it can be seen, 3443 cm^{-1}, 3250 cm^{-1} to 3340 cm^{-1}, 1164 cm^{-1}, and 1065 cm^{-1} peaks are assigned to $–NH_2$ and –OH groups stretching vibration, O−H and N−H stretching vibrations, asymmetric stretching of −C−O−C− bridge, and C−N bond groups in free CS nanoparticles' peak, respectively. For CS-B (NC) sample, the peaks shifting from 1443 to 1440 cm^{-1} is related to strengthening hydrogen bond between CS and A, and the shift from 2916 to 2941 cm^{-1} is attributed to asymmetric C–H stretching owing to the presence of B. Regarding CS-A (C) nanocomposite, 3443 to 3429 and 3422 are recorded because of the formation of strong amid bonds between CS and A and even formation of hydrogen bonds in the compartment of CS-A (C). Moreover, the shift from 1640 to 1651 cm^{-1} (C=O) is revealed after A bonding to CS. The characteristic peaks at around 3200 cm^{-1} and 1356 cm^{-1} (OH stretching vibrations), 1650 cm^{-1}, 1593 cm^{-1}, and 1542 cm^{-1} (owing to aromatic C–C and C–N stretching vibration), and 1223 cm^{-1} and 1086 cm^{-1} (aromatic C–F stretching vibration) are the indicators of Flu CS-A-Flu (NC) and CS-A-Flu (C) samples

vibrations, asymmetric stretching of −C−O−C− bridge, and C−N bond groups in free CS nanoparticles' peak, respectively [25]. Moreover, the characteristic peaks at around 1425 cm^{-1} are recorded due to the presence of C–H stretching in methyl groups of CS nanoparticles, and the stretching vibrations of CH, CH_2, and CH_3 are revealed at around 2800 to 3000 cm^{-1} in CS. The characteristic peaks of C=O, C−N stretching, and C−O stretching vibrations are obtained at around 1640 cm^{-1}, 1383 cm^{-1}, and 1065 cm^{-1} in CS nanoparticles FT-IR peaks [26]. Regarding CS-A (NC) nanocomposite, the peaks shifting from 1443 to 1440 cm^{-1} is related to strengthening hydrogen bond between CS and A, and the shift from 2916 to 2941 cm^{-1} is attributed to asymmetric C–H stretching owing to the presence of A. Another shift from 1640 to 1652 cm^{-1} (C=O) is also related to the presence of A and the formation of CS-A (NC) nanocomposite. For CS-A (C) sample, 3443 to 3429 and 3422 are recorded because of the formation of strong amid bonds between CS and A and even formation of hydrogen bonds in the compartment of CS-A (C). The shift from 1640 to 1651 cm^{-1} (C=O) is also attained after A bonding to CS. Two new peaks at around 1541 cm^{-1} and 1534 cm^{-1} are related to carbonyl groups in the structure of CS-A (C). Generally speaking, the absorption peaks between 3429 and 3500 cm^{-1} are assigned to amide N–H-C=O stretching between CS and A, and 2956 cm^{-1} reveals the presence of methyl groups in the A [27]. The Flu spectrum in the compartment of CS-A-Flu (NC) and CS-A-Flu (C) is corresponded to absorption peaks at around 3200 cm^{-1} and 1356 cm^{-1}, due to OH stretching vibrations, 1650 cm^{-1}, 1593 cm^{-1}, and 1542 cm^{-1}, owing to aromatic C–C and C–N stretching vibration, and 1223 cm^{-1} and 1086 cm^{-1} because of aromatic C–F stretching vibration [28].

DLS, TEM, and SEM Analyses

Without a doubt, the determination of size, dispersity, shape, and morphology of nanocarriers is an undeniable part of every DDS since these features play a momentous impact on the quality of therapeutics delivery to target cells using nanoparticles. As it has been mentioned in various reports, the serum ability of nanocarriers in suppression of target cells, the value of penetration in target cells, biodistribution, the values of used drug dose for treatment, ignoring the human immune systems, and so forth can be profoundly influenced by the size, distribution, shape, and morphology of nanocarrier [29]. As a result, the DLS, TEM, and SEM devices were employed for ascertaining the mentioned physicochemical properties of synthesized nanocomposites (Fig. 2). Practically, the DLS technique was applied for determining the average hydrodynamic diameter, distribution, and polydispersity index (PDI) of CS-based nanocomposites. According to the DLS results in Fig. 2, the average hydrodynamic diameter of CS-A (NC) and CS-A (C) was attained 100 ± 30 (PDI: 0.16) and 150 ±30 (PDI: 0.14), respectively which is desirable for the efficient drug delivery to *C. albicans* cells. Also, the hydrodynamic diameters of CS-A-Flu (NC) (1:1), CS-A-Flu (NC) (1:2), and CS-A-Flu (NC) (2:1) were measured about 100 ± 30 (PDI: 0.17), 150 ±30 (PDI: 0.12), and 100 ± 30 (PDI: 0.13) respectively, while for covalently bonded nanocomposites, the diameters were attained at around 60 ± 20 (PDI: 0.19) for CS-A-Flu (C) (1:1), 150 ± 30 (PDI: 0.16) for CS-A-Flu (C) (1:2), and 150 ± 30 (PDI: 0.18) for CS-A-Flu (C) (2:1). These data indicate that there is a size growth in covalently conjugated nanocomposites which could be due to the weak attachment of TPP between amine groups of chitosan in nanocarrier. For NC samples, TPP can have more effective interaction between positive amine groups in chitosan, and moreover drug encapsulation in the body cavity of the nanocarrier is

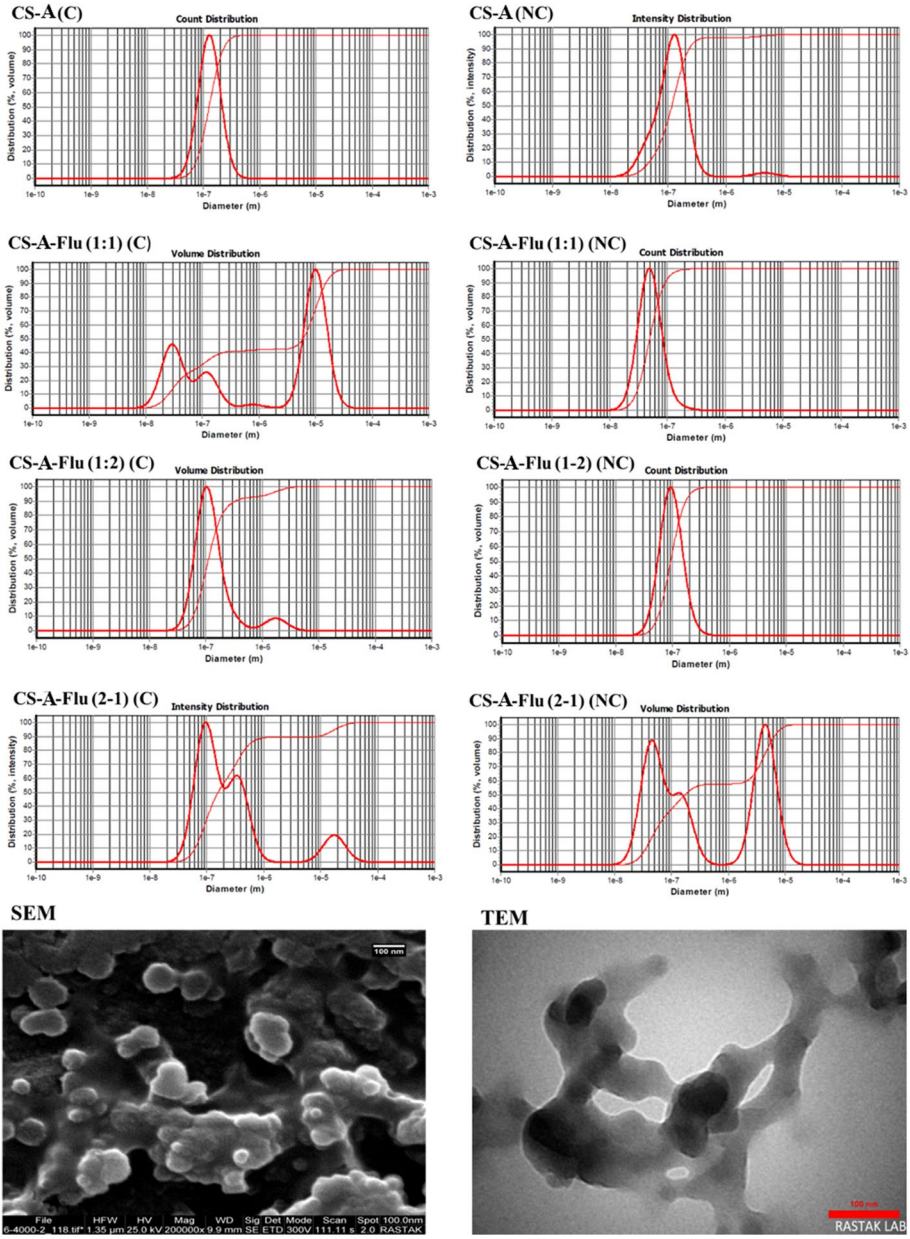

Fig. 2 DLS, TEM, and SEM results of CS-A (NC), CS-A (C), CS-A-Flu (NC), and CS-A-Flu (C). nanocomposites. The average hydrodynamic diameter of CS-based nanocomposites is obtained in the range from 100 to 150 nm using a DLS device. The PDI and distribution of synthesized samples were less than 0.19 which is appropriate for nanocarriers. Based on the TEM image result, a size range from 60 to 100 nm in diameter with approximately a spherical shape and morphology was exhibited for the CS-A sample which was accordingly in line with the image of the SEM device

decreased the amounts of Flu on the surface of the nanocomposite [30]. Moreover, albumin can increase the stability of nanoparticles and also reduce the recognition of nanocarriers by the immune system; PDI values of nanocomposites are presenting a suitable distribution and monodispersity of nanocarriers that are favorable for potent DDS [13].

Meanwhile, the TEM technique was applied to scrutinize the size, shape, dispersion, and structure of the CS-A. Based on the TEM image result, a size range from 60 to 100 nm in diameter with approximately a spherical shape and morphology was acquired for the CS-A sample which was accordingly in line with the image of the SEM device. The unevenness on the surface of nanocomposite could be related to the conjugation of A to the surface of CS nanoparticles. When albumin is attached to chitosan, the resulting nanoparticles have a smoother and glossier surface than chitosan alone [31, 32]. Albumin, an acidic protein, is very soluble and stable in a wide range of pH and for a long time at high temperatures and also in organic solvents which is a suitable subunit for making nanocarriers in drug delivery [15]. Globular and spherical morphology and shape of CS-A in SEM image are shown that this nanocomposite can be used for efficient therapeutic delivery to target cells since the size and morphology of DDSs can facilitate the internalization of nanocarriers into the *C. albicans* cells through various pathways in their walls, such as EPR effect and endocytosis [33].

Antifungal Assay

The antifungal activity of the synthesized samples, including CS-A, CS-A-Flu (NC), CS-A-Flu (C), and Flu were investigated on *C. albicans* ATCC 17110 using the MIC and MFC tests. To evaluate the inhibitory effects of samples, the synthesized nanocomposite was applied to C. albicans ATCC 17110 in various concentrations and ratios (1:1, 1:2, and 2:1). Concentrations of C4 and C5 were attained for MIC and MFC, respectively after treatment with a 1:2 ratio of CS-A-Flu (NC) nanocomposite. These data indicate that non-covalently conjugated CS nanoparticles to Flu can serve as an efficient antifungal therapeutics which could be due to high values of entrapped Flu inside the compartment of CS-A compared to covalently conjugated Flu. Moreover, the positive charge of chitosan amine groups can induce antifungal effects [31]. It has been reported in research works that the main mechanism of CS against microorganisms is the targeting of the cell wall and cell membrane. Chitosan has dual function against bacteria and fungi. Chitosan works as an antibacterial agent by binding to negatively charged bacterial cell walls, altering the permeability of the cell envelope, and then attaching to the DNA to prevent DNA replication. The anti-fungal effect of nanoparticles made of chitosan is achieved similarly by the intimate contact between chitosan and fungal cell membranes, which led to cell membrane disruption [34–36]. Moreover, the MIC and MFC of other CS-based nanocomposites could not be determined since a higher concentration and ratio of Flu is effectively necessary for the suppression of *C. albicans* ATCC 17110. As a matter of fact, *C. albicans* ATCC 17110 was highly susceptible to Flu. The results of our study were in accordance with the findings of Tiboni et al. [35] research in which there was a linear relationship between the concentrations of clotrimazole (as a family of azole drugs) and inhibition of candida species. Chitosan with several biological activities, such as non-toxicity, biocompatibility, biodegradability, ease of chemical modifications, mucoadhesion, anti-inflammatory and wound healing, make CS an advantageous excipient for the vaginal delivery [37].

Biofilm Reduction Assay

The biofilm reduction test was carried out to scrutinize the potency of synthesized nanocomposites (CS-A-Flu (NC), CS-A-Flu (C), and Flu) in the suppression of *C. albicans* ATCC 17110. Different ratios (1:1, 1:2, and 2:1) of the synthesized CS/Flu nanocarriers and pure Flu were employed for the assessment of the specimens' antifungal performance. According to data shown in Fig. 3, CS-A-Flu (NC) (1:1) sample demonstrated more potential ability in inhibition of *C. albicans* ATCC 17110 biofilm (less than 0.05% biofilm formation) compared to other ratios of NC sample, 1:2 and 2:1. The results of biofilm

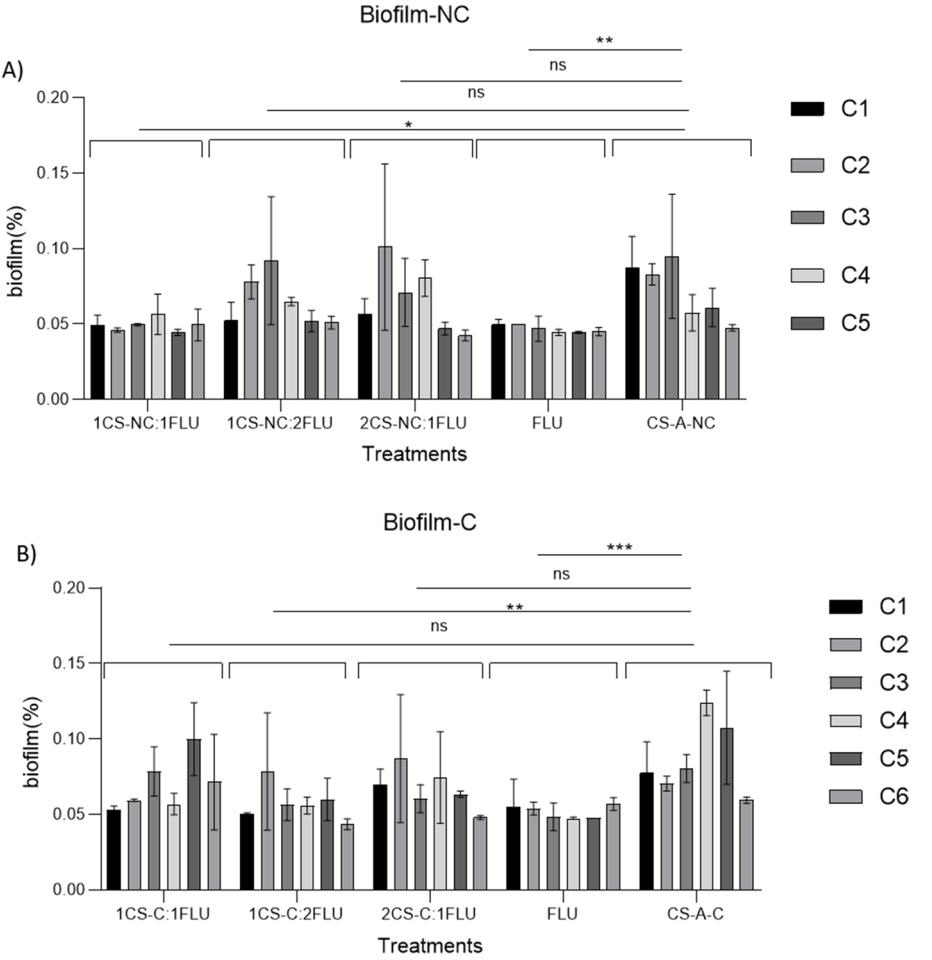

Fig. 3 The results of biofilm reduction activity of CS-A-Flu (NC), CS-A-Flu (C), and Flu on *C. albicans* ATCC 17110 at the ratios of 1:1, 1:2, and 2:1. Based on data, CS-A-Flu (NC) (1:1) sample indicated more potential ability in inhibition of *C. albicans* ATCC 17110 biofilm, with less than 0.05% biofilm formation. The better performance among CS-A-Flu (C) samples was related to CS-A-Flu (C) (1:2) with more than 0.05% biofilm formation. Pure Flu had better biofilm reduction performance compared to all CS-A-Flu (C) samples. Concentration 6 (C6) relatively presented better performance than other concentrations in the reduction of biofilm formation

reduction for free Flu followed a concentration-dependent pattern and totally exhibited the results as same as CS-A-Flu (NC) (1:1) outputs. Furthermore, concentration 6 (C6) relatively demonstrated better performance than other concentrations in reduction and suppression of biofilm formation, while the reverse results were true for C2, C3, and C5. On the other hand, regarding CS-A-Flu (C) nanocomposite and its derivatives, the biofilm reduction ability was generally lower than that of the CS-B-Flu (NC) sample. To put in a more vivid picture, the better performance among CS-A-Flu (C) samples was related to CS-A-Flu (C) (1:2) with more than 0.05% biofilm formation in all concentrations except C6, which was higher than that of CS-A-Flu (NC) and even pure Flu. This result could be due to low drug entrapment efficiency in CS-A-Flu (C) nanocomposites compared with CS-A-Flu (NC) samples which indicates the effects of drug values in nanocarriers [30, 33]. Approximately, the C6 revealed better biofilm reduction activity compared with other concentrations in all CS-A-Flu (C) samples, except CS-A-Flu (C) (1:1) in which C1 was better than others. CS-A (NC) and CS-A (C) samples had lower biofilm reduction ability than other samples which is definitely due to their biocompatibility and lack of Flu in their compartment [9, 21]. Our work outputs were in line with the findings of research by Calvo et al., in which they developed CS-hydroxypropyl methylcellulose tioconazole (member of the azole family) films as an effective anti-candidiasis for treatment of vaginal candidiasis did not lead to considerable hemolytic and cytotoxic effects on the human cells while enough antifungal activity against *C. albicans* which would be used as prominent inhibitory therapeutics against vaginal candidiasis [38]. In another work by Rabey et al., the antimycotic activity of fungal CS (ACT) extracted from *Amylomyces rouxii* and loaded with Flu was evaluated on drug-resistant Candida spp., and results of the MIC test indicated a remarkable antifungal performance for nano-complex while free Flu exhibited weak or no effect against drug-resistant yeast strains which further approves the ability CS-based DDS against Candida species [28]. Complexation of albumin/chitosan improves stability of embedding agents and nanoparticles by increasing the spatial and electrostatic repulsion between the structure of nanoparticles and drug. Moreover, encapsulating Flu as a hydrophobic compound into protein/polysaccharide electrostatic complexes improved solubility of fluconazole and enhance permeation across fungal cell membrane. Furthermore, Chitosan was able to disrupt the biofilm integrity and exhibited antifungal activity against *Candida* species or bactericidal effects against *Pseudomonas aeruginosa* [39].

MTT Assay

The biocompatibility effects of synthesized samples, including CS-A-Flu (NC), CS-A-Flu (C), and pure Flu, were surveyed on HGF normal cells via the MTT assay after 24 h and 48 h of treatment with samples. In this cell viability test, various concentrations and ratios (1:1, 1:2, and 2:1 CS/Flu) of the prepared nanocomposites were investigated. Figure 4 demonstrates the outputs of this test. As it can be seen from the graphs, there is no significant change in the values of cell viability after treatment with various formulations and concentrations, and generally speaking, the CS-A-Flu (C) sample is more biocompatible than the CS-A-Flu (NC) sample which could be due to the high drug content and having more space and cavity in the amounts of loaded-drug, whereas there is a limitation in the conjugation of Flu to CS-A-Flu (C) sample owing to limited available surface groups and lack of enough space for the Flu conjugation [31, 34]. Among samples, Flu alone (85.09% cell viability) exhibited more cytotoxic effects on HGF compared to various ratios of CS-A-Flu (NC) sample after 24h

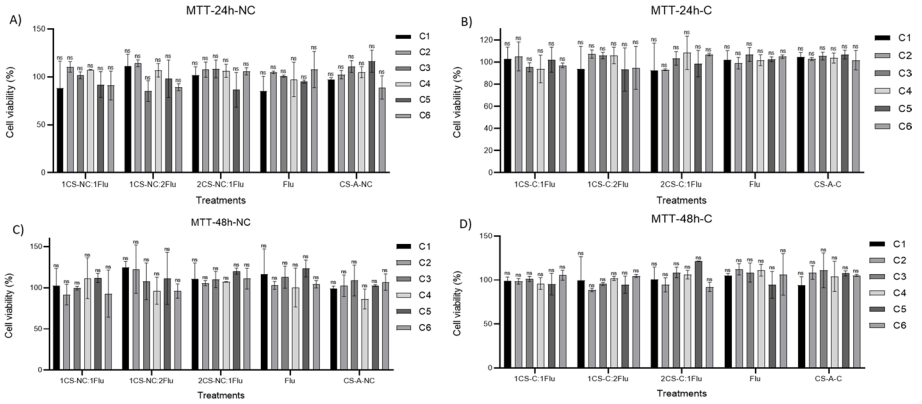

Fig. 4 There is no significant change in the values of cell viability after treatment with various formulations and concentrations, and CS-A-Flu (C) sample is more biocompatible than CS-A-Flu (NC) formulations. Based on graphs, free Flu (85.09% cell viability) exhibited more cytotoxic effects on HGF compared to various ratios of CS-A-Flu (NC) sample after 24h of treatment. The cell viability data of 48 h of treatment revealed a more biocompatibility pattern for CS-A-Flu (NC) formulations as well, even better than that of 24 h of post-treatment. Moreover, CS-A-Flu (C) nanocomposites indicated better biocompatibility than CS-A-Flu (NC) formulations in all ratios and concentrations which could be due to the low values of drug conjugation compared with the loaded drug

of treatment, while more toxicity among CS-A-Flu (NC) ratios is related to C3 in 1:2 ratio of CS/Flu, with about only 14% toxicity. Other concentrations of various ratios did indicate toxicity of more than 11% which reveals the biocompatibility of synthesized samples. The results of 48 h of treatment stated more biocompatibility pattern for CS-A-Flu (NC) formulations as well, even better than that of 24 h of post-treatment. As it is reported, biocompatibility and non-toxicity are the most significant issues with regard to novel nanoparticles-based DDSs [6, 40].

On the other hand, CS-A-Flu (C) formulations showed better biocompatibility than CS-A-Flu (NC) formulations in all ratios and concentrations; for instance, the toxicities of CS-A-Flu (C) formulations on HGF cells are not more than 8% at 24 h of post-treatment. In comparison to a study by Abdellatif et al. [41] in which they develop an efficient localized therapy using sertaconazole nitrate and liposomal nanoparticles for the treatment of vaginal candidiasis, the biocompatibility outputs of their work were completely in line with our findings. Histopathological studies of vaginal samples demonstrated that the histological structure of rat vagina was normal and the mucosa appeared pristine and made up of stratified squamous epithelium rested on the dense sub-epithelial connective tissue with normal blood vessels and without inflammatory cells [41]. The same biocompatibility was observed in the results of research by Calvo et al. [38]. Nikchehreh et al. confirmed the chitosan nanoparticles are biocompatible carriers in gene therapy [32]. Dara et al. evaluated biocompatibility and histopathological of chitosan nanoparticles grafted fish gelatin bio-nanocomposite membranes in vitro and in vivo. In this study the cytotoxicity of bio-nanocomposite membranes was examined using L929 fibroblast cells, and the findings indicated that the membranes were non-toxic and had much greater cell viability percentages than the control [42].

Conclusion

Chitosan with several biological activity, such as antifungal and antibacterial, anti-inflammatory, immuno-enhancing, antioxidant, wound healing, mucoadhesion, and permeation enhancer power properties, make it an ideal candidate for mucosal delivery. To increase the physicochemical qualities and uniformity of CS, as well as to broaden its uses, a CS/albumin derivative was studied, which was created by both chemical changes and the production of polyelectrolyte complexes. Therefore, in this study, we developed covalently and non-covalently bonded CS-albumin (A); then, an ionic gelation technique was developed to prepare chitosan-albumin nanocomposites loaded with Flu antifungals (CS-A-Flu (C) and CS-A-Flu (NC)) to improve the antifungal activity of Flu. This method allows for a controlled electrostatic interaction among cross-linked anionic and polymer cationic groups, resulting in NPs with appropriate dimensions and surface charge. The results have indicated efficient synthesis of nanocarrier with a size range from 60 to 100 nm in diameter. Thereafter, the antifungal activity and biofilm reduction potency were assessed on *C. albicans* ATCC 17110, and potential inhibitory effects were observed for CS-A-Flu (C) and CS-A-Flu (NC) formulations compared with free Flu. The results show both of covalent and non-covalent types of nanocomposites have similar effects on antifungal activity and biofilm reduction potency. The cell viability assay was also implemented on the human normal cells to evaluate the biocompatibility of the synthesized nanocomposite and outputs revealed high biocompatibility of nanocomposites. Based on the results, this nanocomposite would be a potential candidate for the efficient treatment of *C. albicans,* especially against drug-resistant species.

Authors Contribution MHA: study concept and design, acquisition of data, drafting of the manuscript. JM: critical revision of the manuscript for important intellectual content. SK: statistical analysis, administrative, technical and material support, study supervision, analysis and interpretation of data.

Data Availability The data that support the findings of this study are available on request from the corresponding author.

Declarations

Consent to Participate The authors declare that they have consent to participate

Consent for Publication The authors declare that they have consent to publish

Competing Interests The authors declare no competing interests.

References

1. MacAlpine, J., Robbins, N., & Cowen, L. E. (2022). Bacterial-fungal interactions and their impact on microbial pathogenesis. *Molecular Ecology*. https://doi.org/10.1111/mec.16411
2. Carvalho, G. C., et al. (2021). Prevalence of vulvovaginal candidiasis in Brazil: A systematic review. *Medical Mycology, 59*(10), 946–957.
3. Palmeira-de-Oliveira, R., et al. (2022). Women's preferences and acceptance for different drug delivery routes and products. *Advanced Drug Delivery Reviews*, 114133.

4. Kumari, R., Sunil, D., & Ningthoujam, R. S. (2020). Hypoxia-responsive nanoparticle based drug delivery systems in cancer therapy: An up-to-date review. *Journal of Controlled Release, 319*, 135–156.
5. Naderlou, E., et al. (2020). Enhanced sensitivity and efficiency of detection of Staphylococcus aureus based on modified magnetic nanoparticles by photometric systems. *Artificial Cells, Nanomedicine, and Biotechnology, 48*(1), 810–817.
6. Narmani, A., & Jafari, S. M. (2021). Chitosan-based nanodelivery systems for cancer therapy: Recent advances. *Carbohydrate Polymers, 272*, 118464.
7. Chen, Y., et al. (2018). Evaluation of the PEG density in the PEGylated chitosan nanoparticles as a drug carrier for curcumin and mitoxantrone. *Nanomaterials, 8*(7), 486.
8. Niu, S., et al. (2019). A chitosan-based cascade-responsive drug delivery system for triple-negative breast cancer therapy. *Journal of Nanobiotechnology, 17*(1), 1–18.
9. Khakinahad, Y., et al. (2022). Margetuximab conjugated-PEG-PAMAM G4 nano-complex: A smart nano-device for suppression of breast cancer. *Biomedical Engineering Letters, 12*(3), 317.
10. Wang, Y., et al. (2016). Nanoparticles of chitosan conjugated to organo-ruthenium complexes. *Inorganic Chemistry Frontiers, 3*(8), 1058–1064.
11. Kong, M., et al. (2010). Antimicrobial properties of chitosan and mode of action: A state of the art review. *International Journal of Food Microbiology, 144*(1), 51–63.
12. Caraceni, P., et al. (2013). Clinical indications for the albumin use: Still a controversial issue. *European Journal of Internal Medicine, 24*(8), 721–728.
13. Kianfar, E. (2021). Protein nanoparticles in drug delivery: Animal protein, plant proteins and protein cages, albumin nanoparticles. *Journal of Nanobiotechnology, 19*(1), 159.
14. Ogawa, M., et al. (2014). Plasma antithrombin levels correlate with albumin and total protein in gestational hypertension and preeclampsia. *Pregnancy Hypertension: An International Journal of Women's Cardiovascular Health, 4*(2), 174–177.
15. Parodi, A., et al. (2019). Albumin nanovectors in cancer therapy and imaging. *Biomolecules, 9*(6), 218.
16. Wong, C. Y., Martinez, J., & Dass, C. R. (2016). Oral delivery of insulin for treatment of diabetes: Status quo, challenges and opportunities. *Journal of Pharmacy and Pharmacology, 68*(9), 1093–1108.
17. Walke, S., et al. (2015). Fabrication of chitosan microspheres using vanillin/TPP dual crosslinkers for protein antigens encapsulation. *Carbohydrate Polymers, 128*, 188–198.
18. El-Housiny, S., et al. (2018). Fluconazole-loaded solid lipid nanoparticles topical gel for treatment of pityriasis versicolor: Formulation and clinical study. *Drug Delivery, 25*(1), 78–90.
19. Rençber, S., et al. (2019). Formulation and evaluation of fluconazole loaded oral strips for local treatment of oral candidiasis. *Journal of Drug Delivery Science and Technology, 49*, 615–621.
20. Chayachinda, C., et al. (2022). Effect of intravaginal gentian violet for acute vaginal candidiasis treated with a single dose oral fluconazole: A randomised controlled trial. *Journal of Obstetrics and Gynaecology, 42*(6), 2190.
21. Kelidari, H. R., et al. (2017). Improved yeast delivery of fluconazole with a nanostructured lipid carrier system. *Biomedicine & Pharmacotherapy, 89*, 83–88.
22. Faramarzi, N., et al. (2020). Synthesis and in vitro Evaluation of tamoxifen-loaded gelatin as effective nanocomplex in drug delivery systems. *International Journal of Nanoscience, 19*(5), 2050002.
23. Cantón, E., et al. (2003). Minimum fungicidal concentrations of amphotericin B for bloodstream Candida species. *Diagnostic Microbiology and Infectious Disease, 45*(3), 203–206.
24. Fotouhi, P., et al. (2021). Surface modified and rituximab functionalized PAMAM G4 nanoparticle for targeted imatinib delivery to leukemia cells: In vitro studies. *Process Biochemistry, 111*, 221–229.
25. Bandara, S., et al. (2018). Synthesis and characterization of Zinc/Chitosan-Folic acid complex. *Heliyon, 4*(8), e00737.
26. Kaur, K., et al. (2015). Wheat germ agglutinin anchored chitosan microspheres of reduced brominated derivative of noscapine ameliorated acute inflammation in experimental colitis. *Colloids and Surfaces B: Biointerfaces, 132*, 225–235.
27. Tan, W., et al. (2018). Novel cationic chitosan derivative bearing 1, 2, 3-triazolium and pyridinium: Synthesis, characterization, and antifungal property. *Carbohydrate Polymers, 182*, 180–187.
28. El Rabey, H. A., et al. (2019). Augmented control of drug-resistant Candida spp. via fluconazole loading into fungal chitosan nanoparticles. *International Journal of Biological Macromolecules, 141*, 511–516.
29. Yousefi, M., Narmani, A., & Jafari, S. M. (2020). Dendrimers as efficient nanocarriers for the protection and delivery of bioactive phytochemicals. *Advances in Colloid And Interface Science, 278*, 102125.
30. Rezvani, M., et al. (2018). Synthesis and in vitro study of modified chitosan-polycaprolactam nanocomplex as delivery system. *International Journal of Biological Macromolecules, 113*, 1287–1293.

31. Narmani, A., et al. (2018). Targeting delivery of oxaliplatin with smart PEG-modified PAMAM G4 to colorectal cell line: In vitro studies. *Process Biochemistry, 69*, 178–187.
32. Golafzani, F. N., et al. (2022). Delivery of miRNA-126 through folic acid-targeted biocompatible polymeric nanoparticles for effective lung cancer therapy. *Journal of Bioactive and Compatible Polymers, 37*(3), 168–188.
33. Narmani, A., et al. (2020). Breast tumor targeting with PAMAM-PEG-5FU-99mTc as a new therapeutic nanocomplex: In in-vitro and in-vivo studies. *Biomedical Microdevices, 22*(2), 1–13.
34. Fitaihi, R. A., et al. (2018). Role of chitosan on controlling the characteristics and antifungal activity of bioadhesive fluconazole vaginal tablets. *Saudi Pharmaceutical Journal, 26*(2), 151–161.
35. Tiboni, M., et al. (2021). 3D printed clotrimazole intravaginal ring for the treatment of recurrent vaginal candidiasis. *International Journal of Pharmaceutics, 596*, 120290.
36. Meng, Q., et al. (2021). An overview of chitosan and its application in infectious diseases. *Drug Delivery and Translational Research, 11*, 1340–1351.
37. Li, L., et al. (2022). Amphiphilic nano-delivery system based on modified-chitosan and ovalbumin: Delivery and stability in simulated digestion. *Carbohydrate Polymers, 294*, 119779.
38. Calvo, N. L., et al. (2019). Chitosan-hydroxypropyl methylcellulose tioconazole films: A promising alternative dosage form for the treatment of vaginal candidiasis. *International Journal of Pharmaceutics, 556*, 181–191.
39. Silva-Dias, A., et al. (2014). Anti-biofilm activity of low-molecular weight chitosan hydrogel against Candida species. *Medical Microbiology and Immunology, 203*, 25–33.
40. Jabali, M. K., et al. (2022). Design of a pDNA nanocarrier with ascorbic acid modified chitosan coated on superparamagnetic iron oxide nanoparticles for gene delivery. *Colloids and Surfaces A: Physicochemical and Engineering Aspects, 632*, 127743.
41. Abdellatif, M. M., et al. (2020). Formulation and characterization of sertaconazole nitrate mucoadhesive liposomes for vaginal candidiasis. *International Journal of Nanomedicine, 15*, 4079.
42. Dara, P. K., et al. (2021). Biocompatibility and histopathological evaluation of chitosan nanoparticles grafted fish gelatin bio-nanocomposite membranes in rats. *Iranian Polymer Journal, 30*(9), 953–964.